Accepted Manuscript

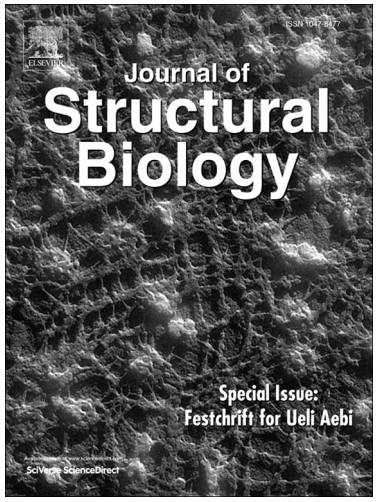

Ocean acidification reduces the crystallographic control in juvenile mussel shells

Susan C. Fitzer, Maggie Cusack, Vernon R. Phoenix, Nicholas A. Kamenos

PII: S1047-8477(14)00183-X
DOI: http://dx.doi.org/10.1016/j.jsb.2014.08.007
Reference: YJSBI 6609

To appear in: *Journal of Structural Biology*

Received Date: 3 July 2014
Revised Date: 17 August 2014
Accepted Date: 24 August 2014

Please cite this article as: Fitzer, S.C., Cusack, M., Phoenix, V.R., Kamenos, N.A., Ocean acidification reduces the crystallographic control in juvenile mussel shells, *Journal of Structural Biology* (2014), doi: http://dx.doi.org/10.1016/j.jsb.2014.08.007

This is a PDF file of an unedited manuscript that has been accepted for publication. As a service to our customers we are providing this early version of the manuscript. The manuscript will undergo copyediting, typesetting, and review of the resulting proof before it is published in its final form. Please note that during the production process errors may be discovered which could affect the content, and all legal disclaimers that apply to the journal pertain.

ACCEPTED MANUSCRIPT

Ocean acidification reduces the crystallographic control in juvenile mussel shells

Susan C. Fitzer*, Maggie Cusack, Vernon R. Phoenix and Nicholas A. Kamenos

School of Geographical and Earth Sciences, University of Glasgow, Glasgow, G12 8QQ, UK

*Tel: +44 (0) 141 330 5442, fax: +44 (0) 141 330 4817, email: susan.fitzer@glasgow.ac.uk.

Keywords: biomineralisation, ocean acidification, temperature, mussels, CO_2, multiple stressors

Abstract

Global climate change threatens the oceans as anthropogenic carbon dioxide causes ocean acidification and reduced carbonate saturation. Future projections indicate under saturation of aragonite, and potentially calcite, in the oceans by 2100. Calcifying organisms are those most at risk from such ocean acidification, as carbonate is vital in the biomineralisation of their calcium carbonate protective shells. This study highlights the importance of multi-generational studies to investigate how marine organisms can potentially adapt to future projected global climate change. *Mytilus edulis* is an economically important marine calcifier vulnerable to decreasing carbonate saturation as their shells comprise two calcium carbonate polymorphs: aragonite and calcite. *M. edulis* specimens were cultured under current and projected pCO_2 (380, 550, 750 and 1000 µatm), following 6 months of experimental culture, adults produced second generation juvenile mussels. Juvenile mussel shells were examined for structural and crystallographic orientation of aragonite and calcite. At 1000 µatm pCO_2, juvenile mussels spawned and grown under this high pCO_2 do not produce aragonite which is more vulnerable to carbonate under-saturation than calcite. Calcite and aragonite were produced at 380, 550 and 750 µatm pCO_2. Electron back scatter diffraction analyses reveal less constraint in crystallographic orientation with increased pCO_2. Shell formation is maintained, although the nacre crystals appear corroded

ACCEPTED MANUSCRIPT

and crystals are not so closely layered together. The differences in ultrastructure and crystallography in shells formed by juveniles spawned from adults in high pCO_2 conditions may prove instrumental in their ability to survive ocean acidification.

Introduction

Global climate change is having a dramatic impact on the oceans which absorb atmospheric CO_2 increasing the partial pressure (pCO_2) and causing ocean acidification. Projections suggest that an increase from 384 µatm to 1000 µatm will result in a reduction of 0.4 pH by the year 2100 (IPCC, 2007; Doney et al., 2009). This ocean acidification poses a threat to those marine calcifying organisms that produce calcium carbonate exoskeletons and shells; due to projected future chemistry changes leading to reduced ocean carbonate saturation state (Ω) (Doney et al., 2009). It is suggested that early life history stages of organisms are most vulnerable to environmental changes (Doney et al., 2009; Byrne, 2012). Impacts of increased pCO_2 on juvenile molluscs include increased mortality, decreased shell deposition and reduced microhardness of oyster *Crassostrea virginica* shells (Beniash et al., 2010; Talmage and Gobler, 2010). Generally, mollusc larvae seem to have reduced survival and shell size when exposed to increased pCO_2 (Byrne, 2012). However, for the newly settled post larvae of the genus *Mytilus edulis*, there was a high tolerance for increased pCO_2 with no impact on survival, but markedly reduced growth and calcification (Thomsen et al., 2013).

Multi-generational studies are a powerful way of assessing the ability of marine organisms to adapt. However such studies remain difficult to address within laboratory conditions. Most studies examine juveniles or adults which have been grown from adults under ambient

ACCEPTED MANUSCRIPT

conditions and transferred to experimental exposure to pCO_2 (Thomsen et al., 2013). Very few multi-generational studies have attempted to study the possibility of adaptation by transferring resistance to pCO_2 from the parent to the gametes (Fitzer et al., 2012; Kurihara and Ishimatsu, 2008), and multi-generational studies have not been undertaken in larger marine invertebrates such as *M. edulis* before. Further long-term and multi-generational study is vital to predict the possibility of acclimation and potential adaptation by marine organisms to future ocean acidification.

The common blue mussel *Mytilus edulis* is an ideal calcifying marine organism for the study of increasing pCO_2, with shell calcium carbonate production comprising both calcite (prismatic layer) and aragonite (nacreous layer, or mother of pearl). As increasing pCO_2 reduces carbonate saturation states within the oceans, aragonite, the less stable polymorph of calcium carbonate, is likely to become more vulnerable to dissolution in comparison to calcite, the more stable polymorph (Doney et al., 2009). In addition, *M. edulis* is an important economical species cultured for food, globally comprising 23.6% (14.2 million tonnes) of an annual $119.4 billion industry (FAO, 2012). Calcifying organisms in general provide a vital carbon sink; as such a shift in carbon usage as a result of increasing pCO_2 could feed back into the climate, reducing the capacity of oceans to absorb atmospheric CO_2.

Physical characteristics such as shell dissolution and reduced growth are one way to examine ocean acidification impacts on marine calcifying organisms (Beniash et al., 2010; Byrne, 2012; Thomsen et al., 2013). Moreover, increased biological stress through increased environmental pCO_2 could also affect shell formation, as well as shell dissolution from external seawater under saturated with respect to carbonate.

ACCEPTED MANUSCRIPT

Here we report the impacts of ocean acidification on second generation juvenile mussels grown for 6 months in experimental culture from spawning of exposed adults. In this study the physical impact of ocean acidification was assessed by examining shell ultrastructure and crystallography in second generation juvenile *M. edulis* grown under current and future projected ocean acidification scenarios (380, 550, 750, 1000 µatm pCO_2).

Methods

Mussel collection and culture.

Mussels (*M. edulis*) were obtained from the Loch Fyne, Argyll, Scotland (Loch Fyne Oysters Ltd) during October 2012. Mussels were placed into experimental tanks (six L) supplied with natural filtered (1 µm and UV) seawater at Loch Fyne temperatures (7 °C) and ambient pCO_2 (~380 µatm). Mussels were fed 10 ml of cultured microalgae (five species of zooplankton, *Nannochloropsis sp*., *Tetraselmis sp*., *Isochrysis sp*., *Pavlova sp*., *Thalassiosira weissflogii* (stock from Reefphtyo, UK,)) per tank every other day. Feeding was conducted during a two week acclimation and throughout the experimental period. Over a six month experimental culture period adults mussels (~1 year old) spawned and juveniles (0.5 – 1 cm) settled onto the six L plastic tank surfaces.

Environmental conditions:

Seasonal experimental temperatures and day length (light) mirrored those at the collection site. Experiments were conducted at 380, 550, 750 and 1000 µatm pCO_2. Seawater pCO_2

ACCEPTED MANUSCRIPT

concentrations were increased up to experimental levels (380, 550, 750 and 1000 µatm pCO_2) over a one month period. CO_2 was mixed into air lines supplying all experimental tanks (Findlay et al., 2008). Gas concentrations were logged continuously using LI-COR® Li-820 CO_2 gas analysers (Table 1). Seawater was topped up with a mixture of seawater and freshwater once a week to simulate fresh water pulses experienced by mussels in their natural environment. This is reflected in calcite (Ω Ca) and aragonite (Ω Ar) saturation states which are similar to other ocean acidification studies examining brackish water environments (Thomsen and Melzner, 2010) and the natural variability present at the collection site (Table 1 Loch Fyne samples). Loch Fyne sample site natural variability for sampling site measurements have been reported in Fitzer et al., (2014). Seawater salinity, temperature, and dissolved oxygen (DO) were checked daily and recorded once a week (YSI Pro2030). Seawater samples were collected (once per month) and spiked with 50 µl of mercuric chloride for subsequent total alkalinity (A_T) analysis via semi-automated titration (Metrohm 848 Titrino plus) (Dickson et al., 2007) combined with spectrometric analysis using bromocresol indicator (Yao & Byrne, 1998) (Smart pH cuvettes, Ocean Optic Ltd) (Hach DR 5000™ UV-Vis). Certified seawater reference materials for oceanic CO_2 (Batch 123, Scripps Institution of Oceanography, University of California, San Diego) were used as standards to quantify the error of analysis (Dickson et al., 2007). Seawater A_T, salinity, temperature and pCO_2 were used to calculate other seawater parameters using CO_2SYS (Riebesell et al., 2007).

ACCEPTED MANUSCRIPT

ACCEPTED MANUSCRIPT

Table 1. Experimental seawater chemistry parameters; salinity, dissolved oxygen (DO), pCO_2, total alkalinity (A_T ± standard deviation from the mean, n=8). Loch Fyne natural seawater was collected from three sites in duplicate for the chemistry parameters reported. Salinity, DO and temperature are averages collected manually throughout experiments, and pCO_2 is the averaged values logged throughout the six months of experiments (logging every five minutes) using LI-COR ® software. Bicarbonate (HCO_3^-) and carbonate (CO_3^{2-}), calcite saturation state (Ω Ca), and aragonite saturation state (Ω Ar) (reported on a log scale) were calculated from measured parameters using CO2Sys.

Experimental condition	**Salinity (ppt)**	**DO (%)**	**Temperature (°C)**	***p*CO$_2$ (µatm)**	**A_T (µmolkg^{-1})**	**HCO_3^- (µmol kg^{-1})**	**CO_3^{2-} (µmol kg^{-1})**	**Ω Ca**	**Ω Ar**
380 µatm Ambient	32.78 ± 1.42	95.58 ± 1.84	9.40 ± 0.36	375.62 ± 9.69	635.24 ± 28.93	590.3	11.9	0.29	0.18
550 µatm Ambient	32.74 ± 1.56	99.04 ± 2.19	10.01 ± 0.56	553.59 ± 62.65	970.76 ± 186.48	908.9	19.7	0.47	0.30
750 µatm Ambient	28.42 ± 4.07	98.64 ± 4.78	10.28 ± 0.34	768.74 ± 41.63	753.64 ± 55.16	725.7	8.4	0.21	0.13
1000 µatm Ambient	34.18 ± 4.58	98.66 ± 1.97	10.23 ± 0.40	1132.53 ± 31.74	698.32 ± 5.77	678.2	5.6	0.13	0.08
Loch Fyne (Average)	19.33 ± 7.46	99.36 ± 12.99	15.70 ± 4.15	341.17 ± 102.57	1261.95 ± 416.39	1170.56 ± 430.42	34.37 ± 18.99	0.88 ± 0.47	0.52 ± 0.29
Loch Fyne (Lowest total alkalinity)	12.80	17.80	11.6	7.95	876.10 ± 12.62	798.39 ± 11.75	29.19 ± 0.44	0.68 ± 0.01	0.39 ± 0.01

ACCEPTED MANUSCRIPT

ACCEPTED MANUSCRIPT

Shell preparation and analysis by Electron Backscatter Diffraction

Electron Back Scatter Diffraction (EBSD) was used to identify calcium carbonate polymorph and determine crystallographic orientation across the middle section of the length of mussel shell at the calcite / aragonite interface. Juvenile mussel shells were carefully prepared as to not damage internal shell layers. Shells were dissected and rinsed to remove tissues with milli-Q water before drying within an oven for 48 hours at 60°C before being embedded into epoxy resin. Resin blocks were polished by hand for 2-4 minutes using grit papers (P320, P800, P1200, P2500, and P4000), followed by further polishing for 4 minutes on cloths using 1 µm and 0.3 µm Alpha alumina, and 2 minutes using colloidal silica to ensure a smooth shell surface. A beam voltage of 20.0 kV was applied under low vacuum mode (~50 Pa) on an FEI Quanta 200F with the stage tilted to 70° to examine backscatter Kikuchi patterns (Pérez-Huerta and Cusack, 2009). Diffraction intensity, phase and crystallographic orientation maps were produced through OIM Analysis 6.2 software. Data points with a confidence index of less than 0.1 were removed. EBSD results are presented as diffraction intensity, phase and crystallographic orientation maps and pole figures with each colour representing a particular crystallographic orientation. Pole figures were examined for spread of crystallographic orientation using 5 degree angle gridlines (Supplementary Figure 1).

Shell etching to reveal ultrastructure

Juvenile mussel shells were prepared and analysed using EBSD, two shells per ocean acidification treatment. Polished shell surfaces were then etched using a commercially available dental paste (Wright Etch Blue, Wright Cottrell) in order to reveal aragonite and calcite crystal

ACCEPTED MANUSCRIPT

structures using SEM. The paste (<200 µl) was placed onto the polished surface of the mussel shell and left for 30 seconds to etch details surrounding the aragonite and calcite crystals. The paste was then wiped away using a lint-free Kim wipe soaked in milli-Q water. The surface was left to dry before coating using an agar gold sputter coater at 5-10 millibar for 120 seconds to prepare for SEM analysis.

Shell lengths

Shell lengths were measured for those juvenile mussel shells embedded in resin for EBSD analyses. Image J was used to measure the length of two shells for each ocean acidification scenario. These two shell lengths were compared using a one-way ANOVA to determine significant differences in growth.

Results

Scanning electron microscopy (SEM) analyses indicates that juvenile mussel shells formed at 380, 550 and 750 µatm pCO_2 comprise both calcite and aragonite, while shells grown under 1000 µatm pCO_2 comprise only calcite (Figure 1). This is confirmed by EBSD phase analyses (Figure 2.iii). SEM imaging revealed slight structural differences, with more uniform crystals of similar size and shape in calcite prismatic layers formed at 380, 550, compared to less organised, thinner and non-uniformly orientated calcite crystals formed at 750 and 1000 µatm pCO_2 (Figure 1). The impact of elevated pCO_2 is evident on the structure of aragonite where the nacreous tablets appear corroded (edges more rounded) and less well packed in shells grown at 550 and 750 µatm

ACCEPTED MANUSCRIPT

pCO_2 (Figure 1). Most striking is the absence of aragonite in shells formed in 1000 µatm pCO_2, having spawned from adults that grew in 1000 µatm pCO_2 conditions.

The diffraction intensity maps (Figure 2.ii) indicate that calcite and aragonite diffract well in these juvenile shells. Calcite diffracts more intensely (brighter) than aragonite. The absence of good diffraction patterns could suggest presence of non-crystalline amorphous calcium carbonate within the shells; this can therefore be ruled out by clearly detected calcite and aragonite observed within the juvenile mussel shells. The crystallographic phase maps (Figure 2.iii) indicate calcite in red and aragonite in green. Aragonite growth is produced in all juvenile shells grown under increased pCO_2, with the exception of 1000 µatm alone (Figure 2.iii). The crystallographic orientation maps (Figure 3.i) show changes in crystallographic orientation from present day (380 µatm) to acidified future projected ocean acidification (750, 1000 µatm) conditions as represented by the colour change (Figure 3.i) corresponding to the colour key. The spread of data points within the pole figures highlight the variation in crystallographic orientation between mussels cultured under increased pCO_2 and the control conditions (Figure 3.ii, and supplementary figure 1). There is less constraint on the calcite crystallographic orientation in juvenile shells grown under increased pCO_2, pole figures highlight spread in the crystallographic orientation of 17.5 degrees at 380 µatm, 35 degrees at 550 µatm, and 20 degrees at both 750 and 1000 µatm (Figure 3.ii, supplementary figure 1). Aragonite crystallographic orientation was also less constrained in juvenile mussel shells grown under increased pCO_2, with increased spread in the crystallographic orientation of 35 degrees at 380 µatm, 40 degrees at 550 µatm, and 62.5 degrees at 750 µatm (Figure 3.ii, supplementary figure 1).

ACCEPTED MANUSCRIPT

Juvenile mussel shell length was also compared between ocean acidification treatments. Shell length significantly decreased (one-way ANOVA, $P<0.045$, F = 6.99, DF = 3) with increasing pCO_2, from 5.90 ± 0.30 mm at 380 µatm, to 3.78 ± 1.29 at 550 µatm, 4.17 ± 0.06 mm at 750 µatm, and 2.92 ± 0.19 mm at 1000 µatm (Supplementary Figure 2, Supplementary Table 1).

Discussion

Scanning electron microscopy analyses indicates that second generation juvenile mussels produce both calcite and aragonite at 380, 550 and 750 µatm pCO_2 but only calcite at 1000 µatm pCO_2. This was supported further by the EBSD analyses. Juvenile *M. edulis* exposed to increased pCO_2 after collection as settled post larvae from the natural environment were observed to have reduced calcification in much higher levels of 3350 µatm pCO_2 (Thomsen et al., 2013). In comparison, juvenile molluscs *Mercenaria mercenaria* and *Argopecten irradians* had increased mortality, and malformation of early shell formation with reduced thickness, integrity and hinge connectedness at much lower levels of pCO_2 comparable to the present study 750 and 1500 µatm (Talmage and Gobler, 2010). However, the results presented here are the first to show calcite-only shells in *M. edulis* juveniles grown from parents exposed to the same conditions. The oyster *Crassostrea virginica* grown from settled post-metamorphosis larvae stage under experimentally increased pCO_2 was also observed to have reduced shell growth (Beniash et al., 2010). Disturbed ultrastructure was also observed in *Mytilus galloprovincialis* (Hahn et al., 2012) after transference to acidified seawater at pH 7.3 compared to ambient at pH 8.1. Under projected ocean acidification scenarios 1000 µatm is expected to arise towards the year 2100 as 'Stabilisation category VI' anthropogenic CO_2 emissions continue (IPCC, 2007; Doney et al.,

ACCEPTED MANUSCRIPT

2009). The lack of aragonite production observed here may have allowed for continued formation of calcite crystals under reduced carbonate saturation states. The outermost calcite continued to grow even when exposed to acidified seawater, whereas internally the aragonite production ceased. This could potentially indicate reduced biological control over biomineralisation of aragonite by the organism, but maintained biological control over the biomineralisation of calcite and potentially raises questions about the integrity of *M. edulis* shells composed of only calcite. Under less severe ocean acidification conditions (550, 750 µatm pCO_2) the nacreous tablets form the usual bricks of the 'brick wall' structure (Marin et al., 2008), although they appear corroded. This could potentially suggest inherited tolerance for moderate pCO_2 levels in second generation mussels compared to those of Talmage and Gobler (2010) that were grown from larvae stages exposed to moderate pCO_2 having being spawned from adults in control conditions. Partially dissolved and thinned nacreous layers and thinned calcitic layers were also observed in *Mytilus galloprovincialis* under naturally acidified conditions (Hahn et al., 2012), which is in agreement with the images presented in this study for *M. edulis*.

The EBSD crystallographic orientation maps and pole figures (Figure 3.i) show reduced constraint in calcite crystallographic orientation in those shells of juvenile mussels grown under increased pCO_2 at 550, 750 and 1000 µatm compared to ambient pCO_2 380 µatm. Less well crystallographically constrained calcite crystals in the juvenile oyster *Crassostrea virginica* under increased pCO_2 may provide a possible explanation as to why such shells have reduced microhardness as observed by Beniash et al., (2010). Since well constrained crystallographic control is a feature of biomineral formation (e.g. Checa et al., 2013; Pérez-Huerta, and Cusack, 2008; Schmahl et al., 2004), diminished crystallographic control may have equally detrimental

ACCEPTED MANUSCRIPT

effects to decreased structural integrity. This possibility should be tested in order to determine the potential influence of OA on shell integrity since reduced crystallographic control may be less apparent yet potentially as damaging as reduced structural integrity.

Juvenile mussel shells lengths were significantly reduced in those mussels grown under increased pCO_2 at 550, 750 and 1000 µatm compared to ambient pCO_2 380 µatm for 6 months exposure. *M. edulis* cultured for 12 months at pH 7.2 were also significantly reduced in shell length (Hahn et al., 2014), whereas earlier shell lengths of *M. edulis* did not show significant differences. The second generation juvenile mussels presented in this study produced significantly smaller at only 6 months in contrast to the findings of Hahn et al., 2014, this could suggest the inherited tolerance for aragonite production at lower pCO_2 at 550, 750 µatm could result in a trade off for shell length.

Conclusion

We present the first study to examine multi-generational impact of ocean acidification on juvenile shell ultrastructure and crystallography of the mollusc *M. edulis*. This study indicates that juvenile mussels are able to produce both aragonite and calcite crystals within the shell in conditions up to and including 750 µatm pCO_2, when grown from adults exposed to the same conditions. For these organisms, 1000 µatm pCO_2 was required for the generation of fully mineralised and normally formed calcite-only shells. This contrasts molluscs which have been grown under ambient conditions until settlement then transferred to experimental conditions which have increased mortality and develop malformed shells at less extreme ocean acidification

ACCEPTED MANUSCRIPT

scenarios 750 µatm pCO_2 (Talmage and Gobler, 2010). This study highlights the importance of multi-generational studies to investigate how marine organisms can potentially adapt to future predicted global climate change. Juvenile mussels exhibit a maintained ability to produce shells when grown from adults exposed to similar experimental conditions which may prove instrumental in their ability to survive ocean acidification.

Acknowledgements

Thanks to John Gillece and Peter Chung at University of Glasgow for technical support. This study was funded by the Leverhulme Trust project entitled 'Biomineralisation: protein and mineral response to ocean acidification' awarded to M.C., N.K. and V.P.

References

Beniash, E., Ivanina, A., Lieb, N. S., Kurochkin, I., Sokolova, I. M. 2010. Elevated level of carbon dioxide affects metabolism and shell formation in oysters Crassostrea virginica. Marine Ecol. Prog. Ser. 419, 95–108.

Byrne, M. 2012. Global change ecotoxicology: Identification of early life history bottlenecks in marine invertebrates, variable species responses and variable experimental approaches. Mar. Environ. Res. 76, 3-15.

Checa, A. G et al., 2013. Crystallographic orientation inhomogeneity and crystal splitting in biogenic calcite. J. R. Soc. Interface. 10, 20130425.

ACCEPTED MANUSCRIPT

ACCEPTED MANUSCRIPT

Dickson, A., Sabine, C. L. & Christian, J. R. 2007. Guide to best practices for ocean CO_2 measurements. PICES Special Publication. 3, 191.

Doney, S. C., Fabry, V. J., Feely, R. A., Kleypas, J. A. 2009. Ocean acidification: The other CO2 problem. Ann. Rev. Mar. Sci. 1**,** 169-192.

Fengzhang, R., Xindi, W., Zhanhong, M., Juanhua, S. 2009. Study on microstructure and thermodynamics of nacre in mussel shell. Mater. Chem. Phys. 114, 367-30.

Findlay, H. S., Kendall, M. A., Spicer, J. I., Turley, C. & Widdicombe, S. 2008. Novel microcosm system for investigating the effects of elevated carbon dioxide and temperature on intertidal organisms. Aquat. Biol. 3, 51-62.

Fitzer, S. C., Caldwell, G. S., Close, A. J., Clare, A. S., Upstill-Goddard, R. C. & Bentley, M. G. 2012. Ocean acidification induces multi-generational decline in copepod naupliar production with possible conflict for reproductive resource allocation. J. Exp. Mar. Biol. Ecol. 418-19, 30-36.

Fitzer, S. C., Phoenix, V. R., Cusack, M., & Kamenos, N. A. 2014. Ocean acidification impacts mussel control on biomineralisation. Sci. Rep. 4 : 6218. doi: 10.1038/srep06218.

Food and Agriculture Organization of the United Nations Annual report. 2012. Fishery and Aquaculture Statistics. ISSN 2070-6057.

Hahn, S., Rodolfo-Metalpa, R., Griesshaber, E., Schmahl, W. W., Buhl, D., Hall-Spencer, J. M. Baggini, C., Fehr, K. T., & Immenhauser, A. 2012. Marine bivalves geochemistry and ultrastructure from modern low pH experiments: environmental effect versus experimental bias. Biogeosciences. 9: 1897-1914.

ACCEPTED MANUSCRIPT

Hahn, S., Griesshaber, E., Schmahl, W. W., Neuser, R. D., Ritter, A-C., Hoffmann, R., Buhl, D., Niedermayr, A., Geske, A., & Immenhauser, A. 2014. Exploring aberrant bivalve shell ultrastructure and geochemistry as proxies for past seawater acidification. Sedimentology. Online ISSN: 1365-3091. doi: 10.1111/sed.12107.

IPCC. Climate Change 2007: the fourth assessment report of the Intergovernmental Panel on Climate Change (IPCC). Cambridge University Press, Cambridge, UK.

Kurihara, H., Ishimatsu, A. 2008. Effects of high CO2 seawater on the copepod (*Acartia tsuensis*) through all life stages and subsequent generations. Mar. Pollut. Bull. 56**,** 1086-1090.

Marie, B., et al. 2011. Nautilin-63, a novel acidic glycoprotein from the shell nacre of *Nautilus macromphalus.* FEBS Journal 278, 2117-2130. doi: 10.1111/j.1742-4658.2011.08129.x.

Marin, F., Luquet, G., Marie, B., and Medakovic, D. 2008. Molluscan Shell Proteins: Primary Structure, Origin, and Current Topics in Developmental Biology Evolution, 80, 209-276, doi: 10.1016/S0070-2153(07)80006-8.

Pérez-Huerta, A., Cusack, M. 2008. Common crystal nucleation mechanism in shell formation of two morphologically distinct calcite brachiopods. Zool. 111, 9-15.

Perèz-Huerta, A., and Cusack, M. 2009. Optimizing electron backscatter diffraction of carbonate biominerals—resin type and carbon coating. Microsc. Microanal. 15, 197–203. doi:10.1017/S1431927609090370.

Riebesell, U., Fabry, V. J., Hansson, L. & Gattuso, J-P. 2007. Guide to best practices for ocean acidification research and data reporting. *Publications Office of European Union, Luxembourg* 1–260.

ACCEPTED MANUSCRIPT

Schmahl, W. W., *et al*. 2004. The microstructure of the fibrous layer of terebratulide brachiopod shell calcite. Europ. J. Mineral. 16, 693-697. doi:10.1127/0935-1221/2004/0016-0693.

Talmage, S. C., Gobler, C. J. 2010. Effects of past, present, and future ocean carbon dioxide concentrations on the growth and survival of larval shellfish. Proc. Natl. Acad. Sci. U.S.A. **107**: 17246-17251.

Thomsen, J., Melzner, F. 2010. Moderate seawater acidification does not elicit long-term metabolic depression in the blue mussel *Mytilus edulis*. Mar. Biol. 157, 2667–2676.

Thomsen, J., Casties, I., Pansch, C., Körtzinger, A., and Melzner, F. 2013. Food availability outweighs ocean acidification effects in juvenile *Mytilus edulis*: laboratory and field experiments. Glob. Change Biol. 19, 1017–1027, doi: 10.1111/gcb.12109.

Figure Legends

Figure 1. Electron microscopy images of the calcite growth of those shells grown under culture at (a) 380 µatm, (c) 550 µatm, (e) 750 µatm, and (g) 1000 µatm. Magnification 10,000x, scale bar = 5 µm for a, c, e and g. Electron microscopy images of the aragonite crystals of those shells grown under culture at (b) 380 µatm, (d) 550 µatm, (f) 750 µatm. Magnification 10,000 x, scale bar = 5 µm for b, d and f. Note there was no aragonite present for 1000 µatm corresponding to image (g).

Figure 2. Secondary electron images and EBSD analyses at calcite (top) / aragonite (bottom) interface of those shells grown under culture at (a) 380 µatm, (b) 550 µatm, (c) 750 µatm, and (d) 1000 µatm. (i) secondary electron image of etched shell at calcite/ aragonite interface after

ACCEPTED MANUSCRIPT

EBSD analyses, (ii) diffraction intensity map (DI) (iii) phase map where calcite is shown in red and aragonite in green, Note that ii – iv all correlate while i does not align properly with ii - iv since shell sections were etched after EBSD analyses and imaged in SEM. Scale bar = 5 µm.

Figure 3. Crystallographic orientation using EBSD analyses for calcite (top) / aragonite (bottom) interface of those shells grown under culture at (a) 380 µatm, (b) 550 µatm, (c) 750 µatm, and (d) 1000 µatm, (i) Crystallographic orientation of calcite crystals in reference to the {0001} plane and aragonite crystals in reference to the {001} plane. Colour keys indicates the coding of the crystallographic planes for calcite; green {0110}, blue {1210}, red {110} planes and for aragonite; green {100}, red {001}, blue {010} planes (Pérez-Huerta and Cusack, 2008). (ii) Pole figures correspond to the crystallographic orientation maps in (iv) and use the same colour key. Upper pole figure of each pair is for calcite (top, 0001 degrees); lower pole figure is for aragonite (bottom, 001 degrees). Scale bar = 5 µm.

ACCEPTED MANUSCRIPT

ACCEPTED MANUSCRIPT

Fig. 1

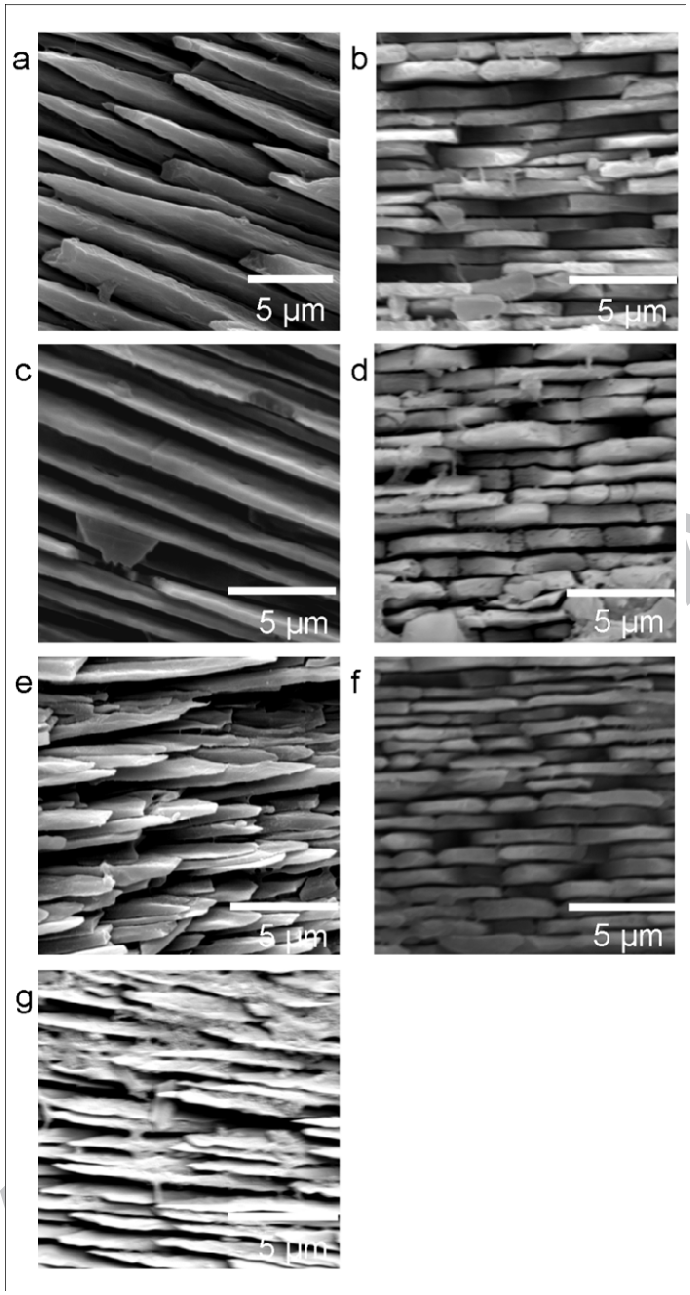

ANUSCRIPT

ACCEPTED MANUSCRIPT

Fig. 2

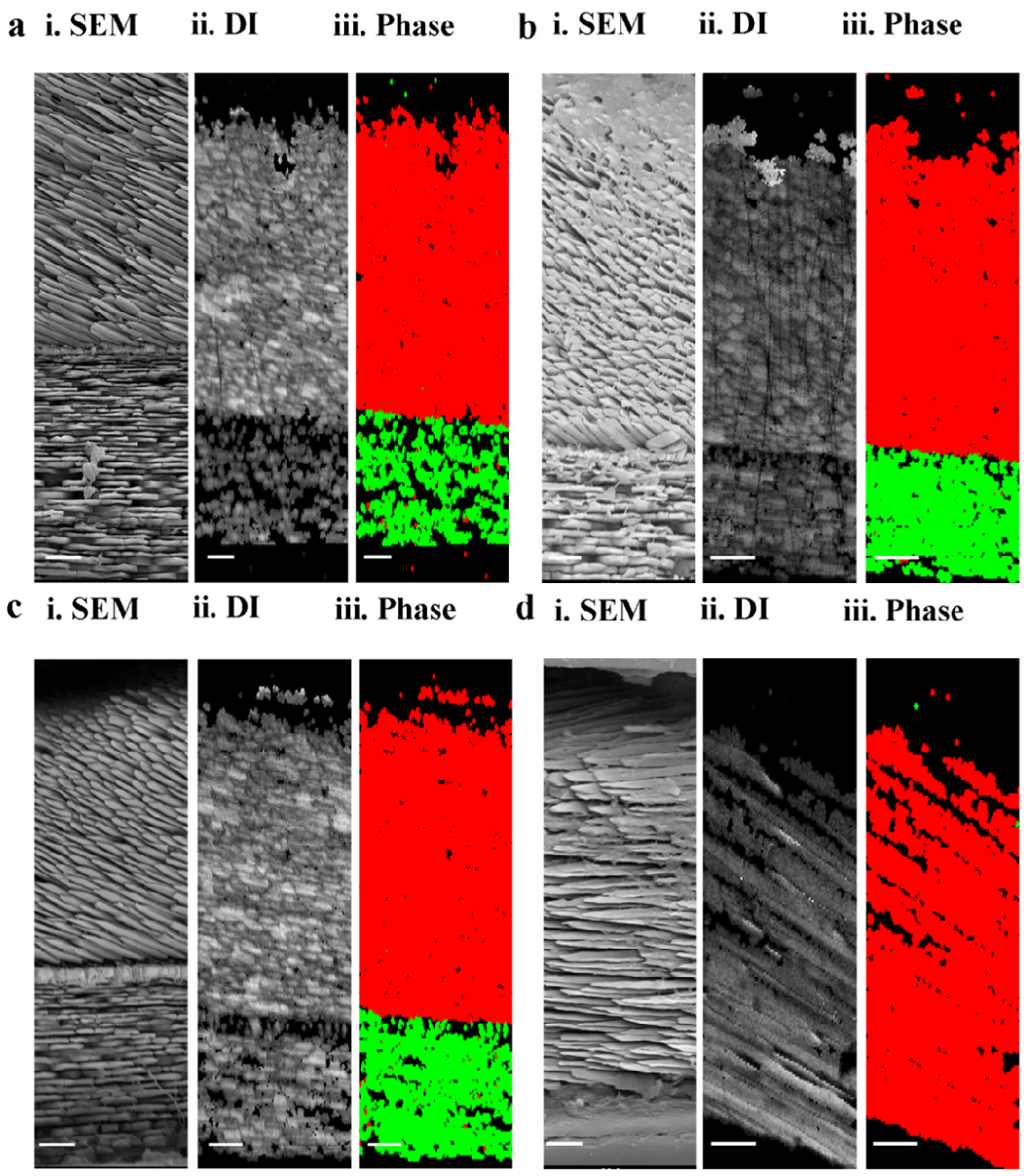

ACCEPTED MANUSCRIPT

Fig. 3